Transactions of the TSME (2015) Vol. 3, No. 1, 22- 28
Journal of Research and Applications in Mechanical Engineering

ISSN 2229-2152 print
DOI: XXXXXXXXXXXXXXXXXX

Research Article

PERFORMANCE OF HIGH-ORDER SCHEMES ON COLLOCATED AND STAGGERED GRIDS

W. Rojanaratanangkule*
A. Hokpunna
Department of Mechanical Engineering,
Faculty of Engineering,
Chiang Mai University,
Chiang Mai 50200, Thailand

ABSTRACT:
Direct numerical simulation of turbulent flows requires tremendous amount of computational power because it is necessary to resolve the spatial structures of the flow down to the Kolmogorov length scale. This procedure generates the so-called grids or meshes. There are two competing grids favour, namely a collocated and staggered grid. To date, it is unclear which one is superior in terms of the resolution power. Recent advance in numerical methods for solving turbulent flows indicates that a staggered grid could be a better candidate for solving turbulent flows due to its superiority in mass-conservation. In order to clarify this possibility, the accuracy of these two grids must be tested using an identical numerical method. In this work, we use a pseudo-spectral method to mimic the behaviour of each numerical approximation. The effects of numerical errors are represented by the modified wavenumber which is then converted back to the physical space. The numerical methods considered in this work are the second-, fourth- and sixth-order central-finite-difference approximations. First a priori error analysis will be investigated, followed by a posteriori error analysis and cross-correlation against the reference solution from the pseudo-spectral scheme. It is found that the second-order scheme on a staggered grid is as good as the fourth-order scheme on a collocated grid which costs twice more expensive.

Keywords: *Direct numerical simulation, high-order method, turbulent flow, homogeneous isotropic turbulence*

1. INTRODUCTION

A computational fluid dynamics (CFD) code used in turbulent research is mostly designed for a structured grid, for example, Cartesian, cylindrical or spherical grids. On these grids, the code developers can use a simple collocated grid, where all the velocities and the pressure sit together at the same position. Alternatively, one can chose a staggered grid where each velocity component sits at different places, as well as the pressure. On one hand, the collocated grid is easy to manage even though it has been shown many times that this type of grid is less accurate than the staggered grid under the same conditions. On the other hand, it is believed that the staggered grid is more accurate and more stable, although one has to pay for additional interpolation and grid management [1]. It is still not clear which one is the better choice in terms of efficiency.

* Corresponding author: W. Rojanaratanangkule
E-mail address: watchapon.roj@eng.cmu.ac.th

In early days, the collocated grid was plagued by the pressure-decoupling problem. This problem was alleviated by the Rie-Chow interpolation [2]. This problem still persists even in a higher-order scheme [3] and it is suggested that using other higher-order approximation of the Poisson equation, rather than the one required by a projection method, seems to help. Furthermore, several research groups [4–5] have developed a fully-conservative scheme that perfectly conserves mass, momentum and energy simultaneously, in spite of having the expense of very wide stencil. However, developing the fully-conservative scheme for the staggered grid is rather difficult. In spite of having fully conservative property which ensures that the numerical simulation will not blow up, the accuracy of higher-order schemes on the collocated grid is not impressive. Gullbrand [6] and Amiri, Hannani & Mashayek [7] found that the second- and fourth-order schemes deliver similar results in the simulation of turbulent channel flow. In contrast to a poor result of the fourth-order scheme on the staggered grid, the compact fourth-order scheme was shown to be much better than the second-order scheme [8]. The result of the second-order scheme with $2.1\text{x}10^6$ grid points can be matched by the fourth-order scheme on $2.6\text{x}10^5$ grid points. It is still not understood why the similar numerical schemes on similar grids can deviate so much by just altering the grid setting from collocation to staggered settings. To answer this question we have to compare the results on the collocated and staggered grids using the same numerical scheme under the same flow conditions and carefully investigate the flow statistics and other important parameters.

In this work, we investigate the decay of homogeneous isotropic turbulence (HIT) using the second-order to sixth-order central-finite-difference approximations (CDAs) and compare the results with those from the pseudo-spectral scheme. The turbulent kinetic energy, velocity-derivative skewness, and longitudinal energy spectra are investigated including the direct comparison with the pseudo-spectral scheme through the cross correlation validation.

2. NUMERICAL APPROACH

The flow considered in this work is governed by the continuity and incompressible Navier–Stokes equations written in Cartesian tensor notation as

$$\frac{\partial u_m}{\partial x_m} = 0 \tag{1}$$

$$\frac{\partial u_m}{\partial t} - \grave{o}_{mjk} u_j \omega_k = -\frac{1}{\rho}\frac{\partial P_{\text{eff}}}{\partial x_m} + \nu \frac{\partial^2 u_m}{\partial x_j \partial x_j} \tag{2}$$

where $x_m = (x, y, z)$ and $u_m = (u, v, w)$ are respectively Cartesian coordinates and the corresponding velocity vector, $\omega_m = \grave{o}_{mjk}\, \partial u_k / \partial x_j$ is the vorticity vector, and $\grave{o}_{mjk}$ is the Levi-Civita symbol. The quantity t denotes time, and $P_{eff} = p + \rho u_j u_j / 2$ includes the thermodynamics pressure and the kinetic energy (the summation over the subscript j being implied). The fluid properties, which are density ρ and kinematic viscosity ν, are assumed constant during the entire simulation.

The simulations were conducted in a periodic cubic box of length 2π. It is thus suitable to Fourier transform the governing equations to perform the spatial derivative. The viscous term is integrated analytically via the use of an integrating-factor technique [9]. The Fourier-transformed Navier-Stokes equations reduce to

$$\frac{\partial}{\partial t}\left(I_v \hat{u}_m\right) = I_v\left(-i\kappa_m \hat{P}_{\text{eff}} + \hat{H}_m\right) \tag{3}$$

where $I_v = \exp\left[\nu \kappa_j \kappa_j t\right]$ is the integrating factor, $\kappa_m = (\kappa_x, \kappa_y, \kappa_z)$ is the wavenumber in each direction of the Cartesian coordinates, $i = \sqrt{-1}$, and $\hat{H}_m$ is the nonlinear term. Equation (3) is advanced in time with a low-storage third-order Runge–Kutta scheme of Spalart, Moser & Rogers [10]. The divergence-free constrain is enforced via a standard pressure-projection method. The product of the nonlinear term, $\grave{o}_{mjk} u_j \omega_k$, is computed in real space and is then dealiased using the 3/2-rule in the Fourier space.

Table 1: Modified wavenumber of central-finite-difference schemes

Scheme	Modified wavenumber $\kappa_m^* \Delta x_m$
Pseudo-spectral	$\kappa_m \Delta x_m$
2nd-order collocated (Col2)	$\sin(\kappa_m \Delta x_m)$
2nd-order staggered (Stg2)	$2\sin\left(\frac{\kappa_m \Delta x_m}{2}\right)$
4th-order collocated (Col4)	$\frac{4}{3}\sin(\kappa_m \Delta x_m) - \frac{1}{6}\sin(2\kappa_m \Delta x_m)$
4th-order staggered (Stg4)	$\frac{9}{4}\sin\left(\frac{\kappa_m \Delta x_m}{2}\right) - \frac{1}{12}\sin\left(\frac{3\kappa_m \Delta x_m}{2}\right)$
6th-order collocated (Col6)	$\frac{3}{2}\sin(\kappa_m \Delta x_m) - \frac{3}{10}\sin(2\kappa_m \Delta x_m) + \frac{1}{30}\sin(3\kappa_m \Delta x_m)$
6th-order staggered (Stg6)	$\frac{75}{32}\sin\left(\frac{\kappa_m \Delta x_m}{2}\right) - \frac{25}{192}\sin\left(\frac{3\kappa_m \Delta x_m}{2}\right) + \frac{3}{320}\sin\left(\frac{5\kappa_m \Delta x_m}{2}\right)$

To mimic the accuracy of each central differencing scheme, the modified wavenumber κ_m^* of each scheme, listed in Table 1, is used instead of the wavenumber κ_m in Eq. (3).

The initial condition for all cases is obtained from the preliminary simulation using the pseudo-spectral method. The prescribed initial spectrum for the preliminary run is

$$E(\kappa,0) = \frac{q^2 \kappa^\sigma}{2A\kappa_p^{\sigma+1}} \exp\left[-\frac{\sigma}{2}\left(\frac{\kappa}{\kappa_p}\right)^2\right] \tag{4}$$

where $\sigma = 2$ is a free parameter, $\kappa_p = 13$ is the location of the peak of the spectrum, $q^2 = 3$ is twice the initial kinetic energy, $\kappa = (\kappa_j \kappa_j)^{1/2}$ is the wavenumber magnitude, and

$$A = \int_0^\infty \frac{\kappa^\sigma}{\kappa_p^{\sigma+1}} \exp\left[-\frac{\sigma}{2}\left(\frac{\kappa}{\kappa_p}\right)^2\right] \mathrm{d}\kappa \tag{5}$$

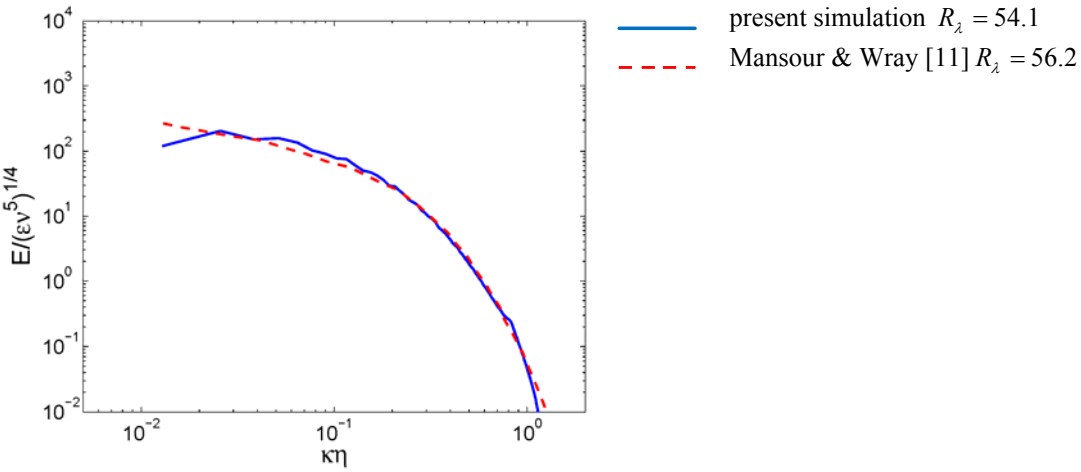

Fig. 1. Energy spectra normalized by Kolmogorov units at t_0.

The preliminary simulation was performed with the resolution of 128^3 and was advanced until $t = 10$ (t_0), at which the realistic HIT develops. It should be noted that the grid used throughout this work is uniform. The energy spectrum at this time agrees very well with that of Mansour & Wray [11] at almost the same Taylor-scale Reynolds number ($R_\lambda = \left(u'u'\right)^{1/2} \lambda / \nu$, where λ is the Taylor's microscale), as illustrated in Fig. 1.

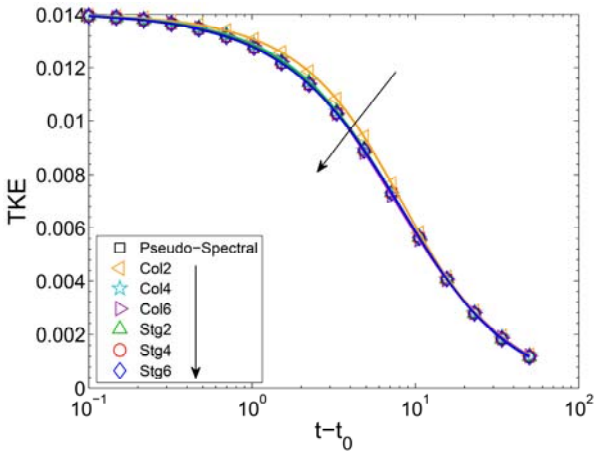

Fig. 2. Histories of turbulent kinetic energy.

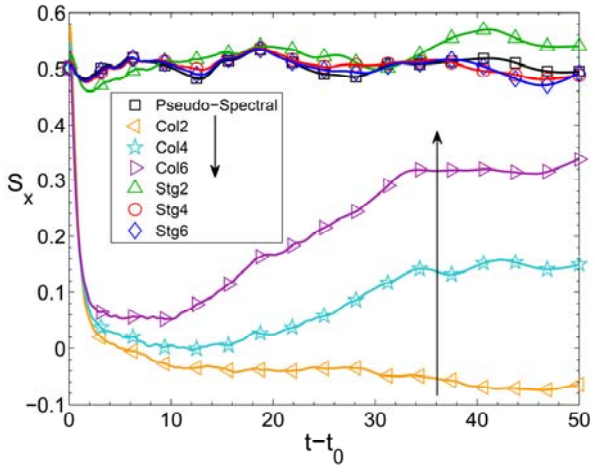

Fig. 3. Histories of velocity-derivative skewness.

3. RESULTS

The turbulent kinetic energy (TKE) is plotted in Fig. 2 showing that the second-order CDA on the collocated grid (Case Col2) deviates clearly from the others. This figure also indicated that the TKE decays slowest with the second-order CDA on the collocated grid (Case Col2), while the others predict practically the same trend. The velocity-derivative skewness is then investigated, as displayed in Fig. 3. Interestingly, the central differencing schemes on the collocated grid predict different third-order statistics of the velocity gradient. Instead of having the values close to 0.5 (a typical value in HIT), the results obtained using the CDAs on the collocated grid deviate greatly from those of the pseudo-spectral scheme. The values of the velocity-derivative skewness first fall sharply to within the range between 0 and 0.1. Note that the arrows indicate the closeness to the spectral scheme. The velocity-derivative skewness of the Case Col2 continues to sink deeper and predicts the negative value of S_x at the end of the simulation. The fourth-order CDA on the collocated grid (Col4) predicts a better value at 0.15 and the value of S_x from the Case Col6 is about 0.34. On the other hand, the results computed by the CDAs on the staggered grid generally agree with the pseudo-spectral method and the values of the skewness swing around 0.5.

This means the velocity gradients predicted by the CDAs on the collocated grid have different distribution than those computed by the pseudo-spectral scheme, and thereby the flows possess different structures.

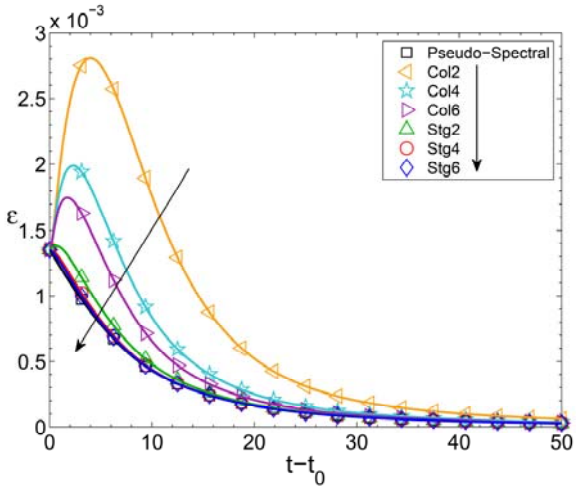

Fig. 4. Histories of dissipation rate.

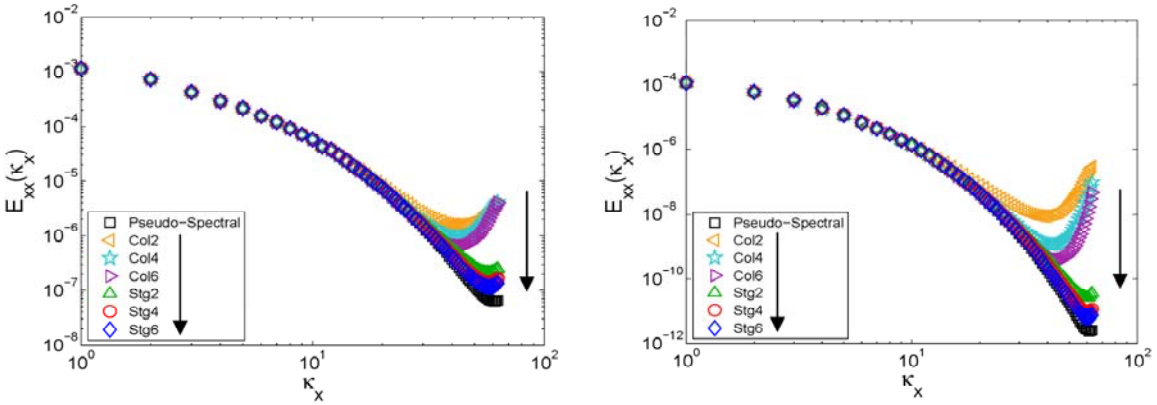

(a) $t - t_0 = 1$ (b) $t - t_0 = 50$.

Fig. 5. Longitudinal velocity spectra.

In theory, the sole source of the reduction in TKE in homogeneous turbulent flow is the turbulent dissipation, ε, which is investigated in Fig. 4. This figure indicates that the exact dissipation rate from the Case Col2 is actually highest. At first glance, it would seem that this plot disagrees with Fig. 2, since one can incorrectly suppose that the dissipation rate of the case Col2 should be lowest due to the highest value of the TKE of this case. In fact, the turbulent dissipation rate is the time derivative of the TKE and the slope of the TKE of the case Col2 is approximately the same to the others in Fig. 2. This leads to the question where the extra dissipation rate comes from. In order to shed some light on this question, the longitudinal velocity spectra after one time unit and at the end of the simulation are plotted in Fig. 5. The plots reveal the energy piles up at the high wavenumber part. Shortly after the simulations started (Fig. 5a), the amplitude of the smallest structure is raised by almost a hundred times. When comparing to the energy of the largest structure, this contributes about 1% of the energy. At the end of the simulation (Fig. 5b), the CDAs on the collocated grid predict the energy of the smallest scale to be 10%. This is a thousand times higher than the true value. Thus, the flow is ultimately changed and the differences lie in the small scale structure. Therefore, the high value of the dissipation rate in Fig. 4 is the result of the increase in the high wavenumber parts of the flow where the dissipation occurs. It is thus now evident that there must be something keeps adding energy to these high wavenumber parts.

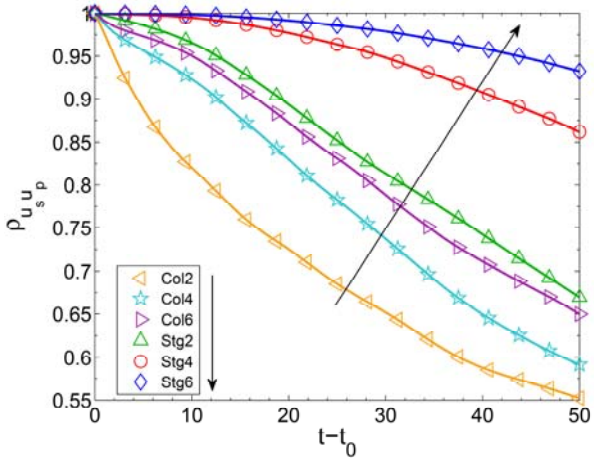

Fig. 6. Cross correlation against the spectral solution.

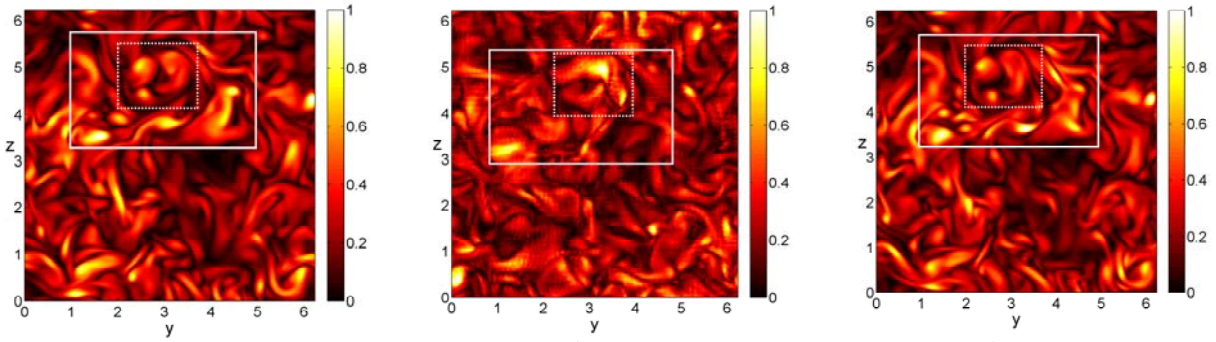

(a) pseudo-spectral method

(b) 2nd-order CDA on collocated grid (Col2)

(c) 6th-order CDA on staggered grid (Stg6)

Fig. 7. Contours of vorticity magnitude at $x = \pi$ and $t - t_0 = 50$.

The goal of CFD is to predict the behaviour of the flow accurately. Ideally, if we know exactly the position, the initial velocity and the forces of all fluid particles in the system, we could ultimately determine the progression of the system. In reality, such information is limited and the incomplete information introduces initial errors to the solution and these errors grow exponentially in time. When the pseudo-spectral scheme is used to simulate the flow, it is certain that the flow can be predicted accurately, at least for a short period of time. When the non-spectral schemes are employed, the numerical errors further widen these errors. Ability to predict the transient flow is very important to many fields such as flow control, disaster mitigation, and fluid structure interaction among others. The investigation of how well the non-spectral schemes follow the prediction of the pseudo-spectral method is next performed. To this end, the cross correlation of the non-spectral schemes against the pseudo-spectral scheme is studied, as illustrated in Fig. 6. It can be seen that the cross correlation of the sixth-order CDA on the collocated grid (Case Col6) is slightly worse than that of the second-order CDA on the staggered grid (Case Stg2). They both predict the flow roughly 65% accurate. The cross correlation of the Case Stg6 is as close as 95% after $t - t_0 = 50$, while that of the Case Col6 drops to the same value at $t - t_0 = 10$.

Next, the contour of the instantaneous vorticity magnitude at the end of the simulation is investigated (Fig. 7). It is clear that the low value of the correlation is the result of the deviation of the predictions. The white box represents a domain containing prominence structures of the flow bounding by the highest vorticity on the bottom left of the box and a large L-shaped vorticity region on the bottom right. The snapshot of the Case Col2 tells different story from the pseudo-spectral scheme and the Case Stg6. The highest vorticity is there but moves slightly to the left. The central dash box shows that the three vortices intermingle and move to the right of the computational box. The L-shaped structured seems to have moved out of this plane ($x = \pi$), while this feature is still present on the Case Stg6 although the left tip curls more inwards than that on Fig. 7(a). We now turn to the more important feature illustrated in Fig. 7(b), which is the wiggles. These wiggles are the physical manifestation of the pile-up of the energy in the

high wavenumber parts seen in Figs. 5(a) and 5(b). The onset of these wiggles is the nonlinear convection term, the second term on the LHS of Eq. (1). The convection process spans over the range $-\pi < \kappa\Delta x < \pi$, while the CDAs on the collocated grid can take only up to $-\pi/2 < \kappa\Delta x < \pi/2$. Therefore, the unresolved waves from the convection term generate aliasing errors in the provisional velocity field. When this field is checked for the mass conservation, the divergence operator of the CDAs on the staggered grid can measure the $-\pi < \kappa\Delta x < \pi$ space, while those on the collocated grid cannot. Therefore the artificial wiggles are further transferred to the pressure field and change the momentum again in the next time step. This feedback mechanism causes the pile-up of the energy to be more severe on the collocated grid than the staggered counterpart.

4. SUMMARY

We show that staggered grid can deliver a better prediction for turbulent flow. The main advantage comes from the ability to correctly detect the mass conservation at the high wavenumber parts. In fact, there are no differences when computing the diffusion term whether using collocated or staggered grids as an analytical integration is employed for this term. For the same order of accuracy, the cost of the convection of u_i in the *i*-direction is exactly the same, while that of the convection of u_i in the *j*-direction is slightly more expensive when using the staggered grid due to additional interpolation. Therefore it is more efficient to use the staggered grid instead of the collocated grid because the result is much more accurate. It should be emphasised that the fourth-order CDA is twice more expensive than the second-order scheme. Therefore, if one wishes to develop a new CFD code, the staggered grid could offer more efficiency than the collocated one.

5. ACKNOWLEDGMENT

We are grateful for the computational resources provided by the Faculty of Engineering, Chiang Mai University and the HPC services from the Large Scale Simulation Research Laboratory of National Electronics and Computer Technology Center.

REFERENCES

[1] Felten, F.N. and Lund, T.S. Critical comparison of the collocated and staggered grid arrangements for incompressible turbulent flows, NASA Technical Report No. ADA412801, 2001.
[2] Rhie, C.M. and Chow, W.L. Numerical study of the turbulent flow past an airfoil with trailing edge separation, AIAA Journal, Vol. 21(11), 1983, pp. 1525-1532.
[3] Henshaw, W.D.A fourth-order accurate method for the incompressible Navier-Stokes equations on overlapping grids, Journal of Computational Physics, Vol.113, 1994, pp. 13-25.
[4] Vasilyev, O.V. High order finite difference schemes on non-uniform meshes with good conservation properties, Journal of Computational Physics, Vol.157, 2000, pp. 746-761.
[5] Verstappen, R.W.C.P. and Veldman, A.E.P. Symmetry-preserving discretization of turbulent flow, Journal of Computational Physics, Vol.187, 2003, pp. 343-368.
[6] Gullbrand, J. An evaluation of a conservative fourth order DNS code in turbulent channel flow, Center for Turbulence Research Annual Research Briefs, 2000, pp. 211-218
[7] Amiri, A.E., Hannani, S.K. and Mashayek, F. Evaluation of a fourth-order finite-volume compact scheme for LES with explicit filtering, Numerical Heat Transfer, Part B, Vol.48, 2005, pp. 147-163.
[8] Hokpunna, A. and Manhart, M. Compact fourth-order finite volume method for numerical solutions of Navier–Stokes equations on staggered grids, Journal of Computational Physics, Vol. 229(20), 2010, pp. 7545-7570.
[9] Rogallo, R.S. (1981). Numerical experiments in homogeneous turbulence, NASA Technical Memorandum 81315.
[10] Spalart, P.E., Moser, R.D. and Rogers, M.M. Spectral methods for the Navier-Stokes equations with one infinite and two periodic directions, Journal of Computational Physics, Vol.96(2), 1991, pp. 297-324.
[11] Mansour, N.N. and Wray, A.A. Decay of isotropic turbulence at low Reynolds number, Physics of Fluids, Vol.(6), 1994, pp. 808-814.